Acta Cryst A FOUNDATIONS ADVANCES

ISSN 2053-2733

Diaphony, a measure of uniform distribution, and the Patterson function

Wolfgang Hornfeck* and Philipp Kuhn

Institut für Materialphysik im Weltraum, Deutsches Zentrum für Luft- und Raumfahrt (DLR), 51170 Köln, Germany. *Correspondence e-mail: wolfgang.hornfeck@web.de

Received 12 December 2014
Accepted 9 April 2015

Edited by H. Schenk, University of Amsterdam, The Netherlands

Keywords: uniform distribution; geometric discrepancy; diaphony; structure-factor equation; Patterson function.

This paper reviews the number-theoretic concept of *diaphony*, a measure of uniform distribution for number sequences and point sets based on a Fourier theory approach, and its relation to crystallographic concepts like the largest interplanar spacing of a lattice, the structure-factor equation and the Patterson function.

1. Introduction

In considering the structure of matter and its elucidation by diffraction experiments, the major focus historically was on the well ordered cases represented by crystals in which atoms, more often than not, arrange themselves into densely packed structures of high symmetry.

Yet, various other states of order exist in-between the ideal crystal and the ideal gas – a statement that remains true even if one restricts oneself exclusively to the solid state – as do various other means of their classification by concepts other than those related to close-packing or symmetry.

One of these concepts, and as yet seemingly more familiar to the mathematician than to the structural chemist or crystallographer, is the notion of *uniform distribution*.

In the first instance, this notion is indeed a purely mathematical one, resting on a principle of fairness. Say, one has a discrete point set falling into a given continuous interval, conveniently chosen to be the unit interval $[0, 1)^d$ for the appropriate dimension d. Uniform distribution is established if any chosen subinterval contains a subset of points whose number matches the value one would expect based on the size of the subinterval used for sampling. The basic idea may be best illustrated by a pictorial representation (Fig. 1). It should be noted, however, that the given definition describes an ideal and limiting case. Although perfect uniform distribution cannot be realized by any *finite* point set, its inevitably existing *irregularities of distribution* can be quantified by suitably chosen geometrical measures, such as the diaphony.

In yet another context, the notion of uniform distribution may be augmented with some additional crystallographic meaning, for instance by emphasizing the common foundations used for the quantitative treatment of uniform distribution as well as for the representation of crystal structures, either by means of their real-space electron density/Patterson function or their reciprocal-space diffraction intensity.

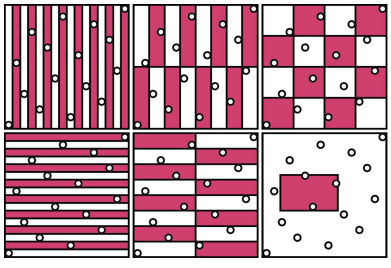

2. On the uniform distribution of atoms in space

A crystal structure comprising N atoms within a unit cell may be abstractly represented by a set $P = \{\mathbf{x}_1, \ldots, \mathbf{x}_N\}$ of N points distributed within the unit cube $[0, 1)^3$. Let

$$e_{\mathbf{h}}(\mathbf{x}) := \exp(i2\pi\langle\mathbf{h}, \mathbf{x}\rangle) \tag{1}$$

denote a complex exponential function of a real-space position vector $\mathbf{x} = (x, y, z)$ and a dual-space index vector $\mathbf{h} = (h, k, l)$, with $\langle\mathbf{h}, \mathbf{x}\rangle$ denoting the usual scalar product, and

$$S_N(e_{\mathbf{h}}, P) = \frac{1}{N}\sum_{j=1}^{N} e_{\mathbf{h}}(\mathbf{x}_j) \tag{2}$$

a corresponding summation over all points. Here, the prefactor $1/N$ effectively represents a scheme of *unit weights*.

Weyl's criterion (Weyl, 1916) states that a sequence of vectors $\mathbf{x}_j \in \mathbb{R}^d$ is *uniformly distributed modulo one*, *i.e.* within the unit hypercube $[0, 1)^d$, if and only if

$$\lim_{N\to\infty} S_N(e_{\mathbf{h}}, P) = 0 \tag{3}$$

holds true for any vector $\mathbf{h} \in \Lambda^* = \mathbb{Z}^d \setminus \{\mathbf{0}\}$, where the specific trigonometric sum $S_N(e_{\mathbf{h}}, P)$ is known as the $\mathbf{h}$-th *Weyl sum*. Note that, here and in the following, all formulas are stated for the general d-dimensional case for which they were originally derived, although their application within a crystallographic context is covered almost exclusively by the case $d = 3$, which is highlighted by our use of three-dimensional vectors $\mathbf{x} = (x, y, z)$ and $\mathbf{h} = (h, k, l)$, whenever we focus on crystal structures and their representation in real and dual space.

Weyl's criterion is furnished with a possibly more intuitive geometric interpretation (see, *e.g.*, Dick & Pillichshammer, 2010, p. 49), schematically illustrated in Fig. 2. It corresponds to mappings of N points x_j in one dimension to the complex unit circle [compare equations (1) and (2)] and the subsequent determination of their centroids, performed for distinct values of h. A balanced distribution of points is achieved, for any given h, in exactly those cases where the centroid coincides with the origin (including degenerate cases in which distinct points coincide in their positions). Now, Weyl's criterion states that the overall degree of uniform distribution can be assessed quantitatively by considering the individual balancings for all h ranging from $-\infty < h < +\infty$ and in the limit $N \to \infty$.

Following Weyl's pioneering work a vast number of measures signifying uniform distribution or deviations thereof have been introduced [see Matoušek (2010) for a concise introduction as well as a more detailed survey given by Hickernell in Hellekalek & Larcher (1998), pp. 109–166, and especially pp. 125–142], among them various mutually related yet distinct concepts known under the general names of discrepancy or diaphony.

Crystallographic applications of *discrepancy* measures were considered by Hornfeck (2013*a*) within a general context of structural chemistry and exemplified by Hornfeck & Kuhn (2014) regarding the description of a low-discrepancy variant of the β-manganese structure exhibiting local octagonal symmetry upon projection.

The concept of *diaphony* (from the Greek term describing dissonance; compare symphony) was introduced by Zinterhof (1976) in order to find a measure for uniform distribution similar in scope to the classical discrepancy measures then existing but by far more tractable from a computational point of view, *i.e.* regarding the computational complexity,

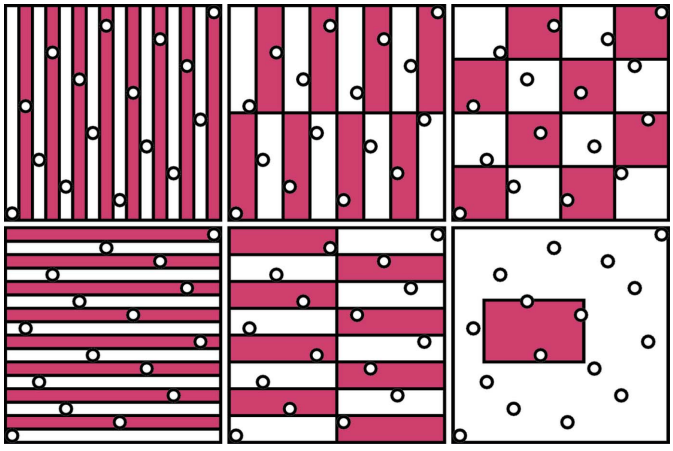

Figure 1
Uniform distribution of a point set, consisting of 16 points in two dimensions. Since its construction relies on van der Corput's one-dimensional sequence, well known for its optimal equidistribution properties [see, *e.g.*, Kuipers & Niederreiter (1974), pp. 127–130], every subinterval of area 1/16 contains exactly one point. One may expand this point of view by replacing the sampling rectangles corresponding to the integer factorizations $1 \times 16 = 2 \times 8 = 4 \times 4 = 8 \times 2 = 16 \times 1$ (top row and bottom left and middle) with generic axis-parallel rectangles (bottom right) up to the point of using arbitrary shapes for sampling, thereby creating a great many real-space measures of uniform distribution summarized under the common name of *geometric discrepancies*.

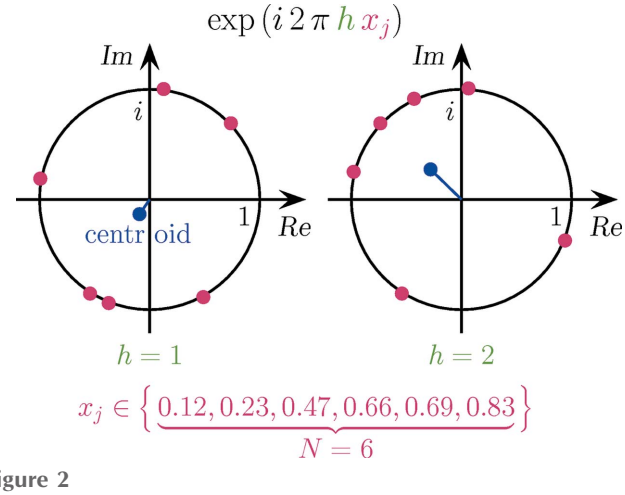

Figure 2
Geometric interpretation of the Weyl criterion. A set of $N = 6$ real numbers is mapped to the complex unit circle *via* the complex exponential $\exp(i2\pi h x_j)$. The image depicts two distinct distributions (red dots) obtained by this mapping for the cases $h = 1$ and $h = 2$, as well as their centroids (blue dots). The position of the centroid, by its vector distance to the origin of the coordinate system, is a case-specific measure for the uniform distribution of the points along the complex unit circle's arc. The Weyl criterion demands the individual balanced distribution for all cases $h \neq 0$ and in the limit $N \to \infty$. The same construction is valid upon replacing the product of the scalar quantities h and x_j for the one-dimensional case with the scalar product of their vectorial counterparts $\mathbf{h}$ and $\mathbf{x}_j$ in higher-dimensional ones.

depending on the number of points N and the dimension of space d, involved in its calculation. Indeed, the computational complexity for the diaphony is $\mathcal{O}(d \cdot N^2)$ while it is $\mathcal{O}(N^d)$ for the discrepancy (Hellekalek & Niederreiter, 1998).

Another distinction between discrepancy and diaphony measures is due to their construction in real and dual space, respectively. Although definitions may be phrased in either space interchangeably, some choice often seems more natural than others in distinct contexts, either depending on some required property of the measure (*e.g.* translation invariance) or having some specific application in mind.

Now, Zinterhof's *diaphony* (Zinterhof, 1976) is defined as

$$F_N(P) = \left[\sum_{\mathbf{h}\in\Lambda^*} r(\mathbf{h})^{-2} \cdot \left|S_N(e_{\mathbf{h}}, P)\right|^2\right]^{1/2}, \qquad (4)$$

where

$$r(\mathbf{h}) = \prod_{j=1}^{d} \max\left(1, |h_j|\right) \qquad (5)$$

is a weight function based on the index vectors $\mathbf{h}$ with the h_j denoting their components. Stated in technical terms, Zinterhof's diaphony represents a weighted L^2 norm of the Weyl sum $S_N(e_{\mathbf{h}}, P)$, which itself is given by a weighted trigonometric sum of the point set P under consideration (see Appendix *A* for more remarks on various notions of norms and weights), which in turn is uniformly distributed in $[0, 1)^d$ if and only if

$$\lim_{N\to\infty} F_N(P) = 0. \qquad (6)$$

Note that the sum of squares given in Zinterhof's formula for the diaphony [equation (4)] approaches zero asymptotically, as N tends to infinity, if and only if this holds true for any of its summands, thereby fulfilling Weyl's criterion [equation (3)].

In the following we will show, mainly as a review and crystallographic interpretation of existing results in metric number theory, that specific choices of the norm and weights, distinct from the aforementioned ones, have their well known crystallographic counterparts and thereby confer a general crystallographic meaning to the concept of diaphony as well.

3. A diaphony with specific L^P norm: the largest interplanar spacing of a lattice

The *spectral test* introduced by Coveyou & MacPherson (1967),

$$\sigma(L) = \frac{1}{\min_{\mathbf{h}\in\Lambda^*}|\mathbf{h}|}, \qquad (7)$$

is a figure of merit that is especially useful for the quantitative assessment of linear and multiplicative congruential random-number generators (Hellekalek & Larcher, 1998, pp. 49–108), due to their intrinsic sublattice structure [on which basis Hornfeck & Harbrecht (2009) and Hornfeck (2012, 2013*b*) discuss crystallographic applications of multiplicative congruential generators].

Now, the outcome of equation (7) has a crystallographic interpretation as it yields the maximal distance, $\max d_{hkl}$, between adjacent parallel net planes (hkl), in which the maximum is taken over all families of net planes spanning a crystal's lattice (Fig. 3; see, *e.g.*, Hellekalek & Larcher, 1998, pp. 79–89). Note that, in contrast to this real-space geometric interpretation, the spectral test, as its name suggests, really works in dual space, determining the length, *i.e.* the Euclidean norm $|\mathbf{h}| = (h^2 + k^2 + l^2)^{1/2}$, of the shortest, non-vanishing Miller index vector $\mathbf{h} \in \Lambda^*$ and returning its reciprocal value.

While this classical spectral test thus by design only works for *lattice* point sets L, a variant employing weighted Weyl sums $S_N(e_{\mathbf{h}}, P)$ is applicable for *general* point sets P with or without an underlying lattice structure:

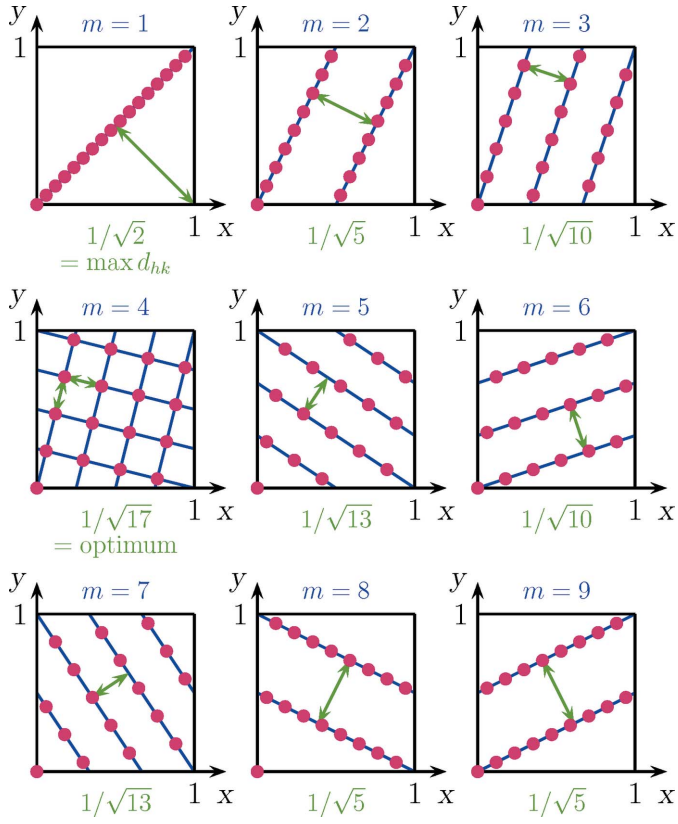

Figure 3
Geometric interpretation of the spectral test. Depicted is a series of point patterns consisting of 17 nodes each (red dots) generated by the multiplicative congruential method. Hence, the fractional coordinates of all nodes within a unit square $[0, 1)^2$ are represented as $(x, y) = (X, Y)/17$ with their integral coordinates (X, Y) related as $Y = mX \pmod{17}$, *i.e.* *via* a multiplication followed by a division with a remainder. While X runs smoothly from 0 to 17, tracing out a torus line of slope m, a sublattice structure is generated with every integral value of X creating a node. Now, any given set (h, k) of parallel lines in a two-dimensional lattice is characterized by its perpendicular interplanar spacing d_{hk}. A maximum value $\max d_{hk}$ will be taken for the unique set featuring a maximum density of lattice points along its parallel lines, thereby specifying the distribution properties of the nodes within a given sublattice designated by m. Note that $\max d_{hk}$ diminishes for increasing values of m until it reaches a global minimum for $m = 4$, the case of a square sublattice with an optimum uniform distribution of its nodes (since the cases with $m = 9 + n$ are mirror images of the ones with $m = 8 - n$, with respect to the y axis, an equivalent solution is given by $m = 13$).

$$\sigma_N(P) = \sup_{\mathbf{h}\in\Lambda^*} \left| \frac{S_N(e_\mathbf{h}, P)}{r(\mathbf{h})} \right|. \tag{8}$$

Again, as

$$\lim_{N\to\infty} \sigma_N(P) = 0 \tag{9}$$

holds true for point sets satisfying Weyl's criterion, $\sigma_N(P)$ is a measure of uniform distribution. For the special case of lattice point sets L the Weyl sum becomes

$$S_N(e_\mathbf{h}, L) = \begin{cases} 1 & \text{for } \mathbf{h} \in \Lambda^* \\ 0 & \text{otherwise} \end{cases}, \tag{10}$$

thereby reducing the general definition of equation (8) to the particular one of equation (7), *i.e.* for the choice of $r(\mathbf{h}) = |\mathbf{h}|$.

Moreover, identifying

$$T(P) = \left[\frac{S_N(e_\mathbf{h}, P)}{r(\mathbf{h})} \right]_{\mathbf{h}\in\Lambda^*} \tag{11}$$

emphasizes that the spectral test for general point sets

$$\sigma_N(P) = \left\| T(P) \right\|_\infty, \tag{12}$$

applying the L^∞ norm, is merely a variant of Zinterhof's diaphony

$$F_N(P) = \left\| T(P) \right\|_2, \tag{13}$$

applying the L^2 norm, instead (Hellekalek & Larcher, 1998, p. 90). Contrariwise, Zinterhof's diaphony can be conceived as a *weighted spectral test* (Hellekalek & Niederreiter, 1998). These interrelations of the diaphony with the spectral test and other measures of uniform distribution are explored in greater detail by Dick & Pillichshammer (2005), while generalized, hybrid variants of the spectral test are discussed by Hellekalek (see a corresponding chapter in Kritzer *et al.*, 2014).

4. A diaphony with specific inner weights: the structure factor

While Zinterhof's original definition of the diaphony employed unit weights of $1/N$ in the expression of the exponential sum $S_N(e_\mathbf{h}, P)$, this was subsequently extended (Lev, 1995) to non-negative real weights, $\rho_j \geq 0$, yielding a generalized diaphony,

$$F_N(P) = \left[\sum_{\mathbf{h}\in\Lambda^*} r(\mathbf{h})^{-2} \cdot \left| \sum_{j=1}^{N} \rho_j \cdot e_\mathbf{h}(\mathbf{x}_j) \right|^2 \right]^{1/2}, \tag{14}$$

instead.

Applying only a slight change of notation, the kind of exponential summation proposed by Lev is analogous to the one applied by crystallographers in the *structure-factor equation*:

$$F_\mathbf{h} = \sum_{j=1}^{N} f_j \cdot e_\mathbf{h}(\mathbf{x}_j), \tag{15}$$

in which the weights are replaced, most naturally, by the atomic form factors f_j.

The structure factor denotes the relation of a given crystal structure to its diffraction pattern, in which physical atoms replace mathematical points in real space while the mathematician's dual lattice Λ^* is represented by the crystallographer's reciprocal one. Specifically, a crystal structure's representation in real and dual space is interrelated *via* a Fourier transform,

$$\varrho(\mathbf{x}) = \frac{1}{V} \sum_{\mathbf{h}\in\Lambda^*} F_\mathbf{h} \cdot e_\mathbf{h}(\mathbf{x})^{-1}, \tag{16}$$

based on structure factors. Here, $\varrho(\mathbf{x})$ is the real-space electron density (continuous in $\mathbf{x}$).

In fact, more commonly it is the *inverse problem*, *i.e.* to deduce a crystal's structure, the specific arrangement of its atoms in space, from its experimentally observable diffraction pattern, that attracts the attention of the crystallographer [indeed, the current definition of a crystal relies solely on the appearance of its diffraction pattern, namely its 'essential discreteness'; for a treatment of *mathematical diffraction theory* which covers the subtleties, and to some extent necessities, of such rather imprecise definitions see Baake & Grimm (2011, 2012)]. This inverse problem is greatly complicated by the structure factor being a complex quantity, *i.e.* a *phasor* $F_\mathbf{h} = |F_\mathbf{h}| \exp(i\varphi_\mathbf{h})$, composed of a complex modulus (amplitude) $|F_\mathbf{h}|$ and a complex argument (phase) $\varphi_\mathbf{h}$. The intensity $I_\mathbf{h}$, however, as the observable of a diffraction experiment, is related to the square of the modulus, *i.e.* $I_\mathbf{h} \propto |F_\mathbf{h}|^2$. Thus, while the amplitude $|F_\mathbf{h}|$ of a structure factor can be easily recovered from a scattering experiment, its phase $\varphi_\mathbf{h}$, exceedingly more important for the reconstruction, is lost, resulting in the so-called *phase problem of crystallography*.

Notwithstanding, from the aforementioned similarity between the weighted Weyl sum and the structure-factor equation and the well known fact that $|F_\mathbf{h}|^2 \propto I_\mathbf{h}$, it is immediately clear that a crystallographic measure for the uniform distribution of atoms in space could be based on a *diaphony on intensities* (or calculated/observed squared structure factors for that matter).

One should note, however, a subtle yet inevitable difference in the number-theoretic and crystallographic definitions. Whereas the number-theoretic case features a point set as a sum of delta distributions, this is replaced by a sum of *spatially extended* atoms in the crystallographic case. In particular, this affects the specific nature of the inner weights, regarding their dependency on the dual-space scattering vector – which is a constant for each point scatterer in the case of Lev's weights (*i.e.* corresponding to a real-space delta distribution after Fourier transformation) but varying with $(\sin\theta)/\lambda$ in the case of the atomic form factors. Naturally, this difference is mirrored in the measured intensities, or its corresponding diaphony, too.

5. Sketches of uniform distribution I: special cases

In the following we would like to convey some of the aforementioned ideas by amending the previous quantitative

mathematical definitions with more qualitative views regarding their crystallographic interpretation. For this purpose we illustrate some exceptional as well as general cases with respect to their uniform distribution properties. All the sketches shown depict the real-space distributions of point scatterers placed within the interval $(x, y) \in [0, 1)^2$ (a crystallographer's unit cell in two dimensions, x to the right, y upwards; Figs. 4 to 6, top) with their respective diffraction patterns in reciprocal space restricted to the interval $(h, k) \in [-7, 7]^2$ (k to the right, h downwards; Figs. 4 to 6, bottom). In order to evoke some intuition we choose to compare three pairs of limiting cases and their characteristics contrasting each other.

First, let us consider the simplest realization of a discrete point set: a single point, representing a crystal structure, periodic in two dimensions, consisting of one atom per unit cell (Fig. 4, left). Irrespective of its exact location within the real-space unit cell its diffraction pattern in reciprocal space remains invariant and, in fact, *equidistributed* with respect to the intensity associated with any scattering vector **h**. On the other hand, the ideal case of uniform distribution is given by a continuous density distribution of scattering matter (Fig. 4, right). In Fourier space this corresponds to a single δ-peak at the origin, representing the average scattering magnitude. In the special case of X-ray diffraction the structure factor F_{00} yields the total number of electrons per unit cell. Both cases represent the limiting cases of uniform distribution – although one may wonder why they appear different in the first place, since the Fourier transform of a single peak in real space yields a uniform distribution in reciprocal space, and *vice versa*. The reason for this is that the depicted real-space point patterns always have to be extended periodically (especially noteworthy regarding the top-left part of Fig. 4), *i.e.* only the unit cells of the point patterns are depicted, while, on the other hand, the *intensity-weighted* reciprocal lattice lacks translational symmetry.

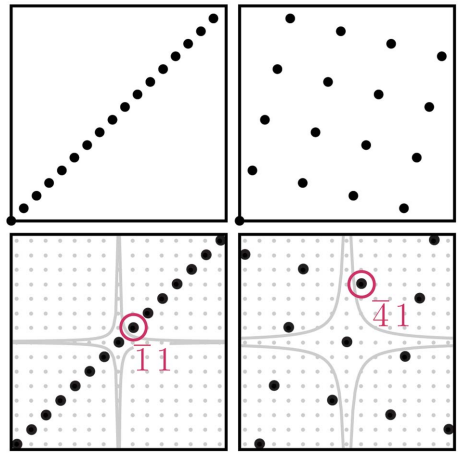

Figure 5
Special cases of uniform distribution I: the spectral test for sublattices. Reviewing the cases $m = 1$ and $m = 4$, as presented in Fig. 3, it turns out that the amount of area enclosed by the hyperbolas $|h \cdot k| = \varepsilon(m)$ (depicted in grey) for some $\varepsilon(m) > 0$ – while adapting to the shortest, non-vanishing reflection hk closest to the origin – differs for the cases $m = 1$ and $m = 4$, thereby matching the different degree of uniform distribution found in the corresponding (lattice) point set. Note that the nodes of the reciprocal lattice are highlighted by small solid circles in grey and should not be confused for reflections.

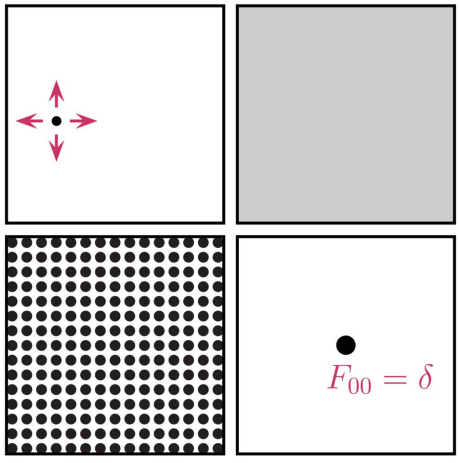

Figure 4
Limiting cases of uniform distribution: discrete *versus* continuous distributions. In a way both cases represent a uniform distribution, either with respect to the intensity distribution found in reciprocal space (discrete case) or regarding the homogeneous density in real space (continuous case). Here, the discrete case is represented by a single point scatterer (and its translated copies outside the depicted frame), where the red arrows are meant to indicate that the intensity distribution is independent of the exact position of the scatterer within the unit cell. Note that the continuous case of uniform distribution is characterized by the presence of a single δ-peak at the origin and the absence of intensity elsewhere. This tell-tale feature of uniform distribution cannot be realized in the discrete case, except for some finitely bounded region about the origin of reciprocal space (compare Figs. 5 and 6).

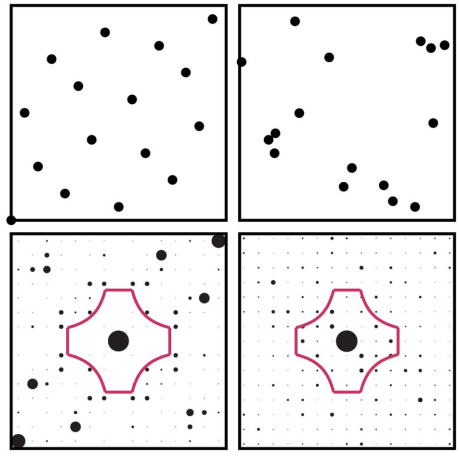

Figure 6
Special cases of uniform distribution II: quasi-random *versus* pseudo-random point sets. Note the comparative absence or presence of point clustering and void formation for the quasi-random and pseudo-random point set, respectively, as well as the comparative absence or presence of intensity close to the origin. In particular, a single contour line is shown (depicted in red), corresponding to the weight function $r(\mathbf{h}) = \max(1, |h|) \cdot \max(1, |k|)$ used in the definition of the diaphony, highlighting a region of vanishing intensity in the quasi-random case. As an aside, the anisotropy of the product weights as defined in equation (5) is visible: the 'octagonal' shape of the contour line, featuring alternating planar and concave edges, indicates the decay of the weights proceeding as $1/r^2$ along the axes and as $1/r^4$ along the diagonals, with r denoting the radial distance from the origin.

Second, we consider the special cases of point sets with a sublattice structure. As mentioned before, a measure of uniform distribution for these point sets is given by the spectral test. While we focused on the largest interplanar spacing of a lattice before, we now show its relation with the diffraction pattern. For this purpose we compare the diffraction patterns of the sublattices generated by the multiplicative congruential generators $Y = mX \pmod{17}$ and consisting of 17 points for the cases $m = 1$ (Fig. 5, left) and $m = 4$ (Fig. 5, right). As expected, and demanded by the very definition of the spectral test, the non-vanishing reflection observed closest to the origin specifies the uniformity of distribution *via* its Euclidean norm $|\mathbf{h}| = (h^2 + k^2)^{1/2}$. Since $|\mathbf{h}| = 2^{1/2}$ for $h = -1, k = 1$ in the case $m = 1$ and $|\mathbf{h}| = 17^{1/2}$ for $h = -4, k = 1$ in the case $m = 4$ the spectral test yields $\sigma(m = 1) = 1/2^{1/2} \simeq 0.707$ and $\sigma(m = 4) = 1/17^{1/2} \simeq 0.243$, respectively, thereby qualifying the case $m = 4$ as the one being more uniformly distributed (compare Fig. 3). This outcome may be illustrated in another way, namely by a representation of the different extent to which the region close to the origin features an absence of intensity (Fig. 5; compare Matoušek, 2010, p. 74).

Third, we consider the special cases of quasi-random and pseudo-random point sets. The chosen quasi-random point set, consisting of 16 points (Fig. 6, left), corresponds to the one constructed from the van der Corput sequence already mentioned in §1. The pseudo-random point set represents 16 random points according to the random-number generator implemented in *Mathematica* (Fig. 6, right). From their diffraction patterns some differences can be spotted regarding the occurrence of comparatively stronger intensities for higher-order reflections for the quasi-random case with respect to the pseudo-random one and, more importantly, a different extent of vanishing intensity close to the origin. This is a signature of the different degree of uniform distribution, since the diaphony is lower in those cases for which the intensity closer to the origin is diminished, thereby precluding strong reflections occurring in this region for quasi-random point sets.

6. Sketches of uniform distribution II: the general case

Overall, and despite the given examples, it does not appear to be easy to find a general relation between the uniform distribution of atoms in space, the corresponding value of the diaphony and the total intensity distribution resulting from a diffraction experiment.

A suitable approach, in our opinion, is to treat this question in the context of a *sampling problem*. Then, a qualitative impression is based on the idea that the plane waves $e_{\mathbf{h}}(\mathbf{x}_j)$ used in the definition of the diaphony and the net planes (hkl) occurring in a crystal likewise scan their corresponding discrete structures spatially, irrespective of whether they are composed of abstract points or actual atoms. For any given family of plane waves or net planes, a specific sampling interval along the perpendicular direction corresponds to the wavelength of the plane waves or the interplanar spacing d_{hkl} of the net planes.

In those cases where the interplanar spacing d_{hkl} matches the array of atoms (points), up to the case of being in perfect registry, a considerable probability exists for the corre-

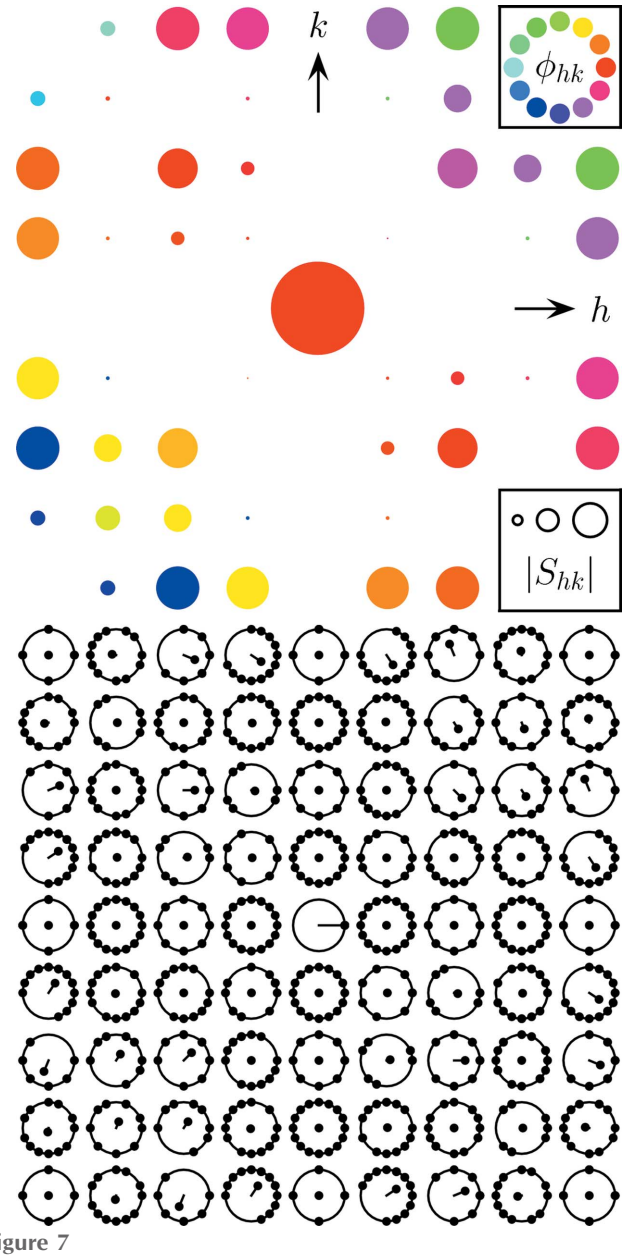

Figure 7
Weyl sum representation of structure factors I: comparison of a conventional plot of the amplitude $|S_{hk}|$ and phase φ_{hk} of a unit-weight structure factor $S_{hk} = 1/N \cdot \sum_{j=1}^{N} e_{hk}(\mathbf{x}_j)$ calculated for the $N = 16$ van der Corput point set in two dimensions (top; compare Fig. 1) with a second one emphasizing the uniform distribution for a given index pair h and k using the geometric interpretation of the Weyl criterion (bottom; compare Fig. 2). The values of amplitude $|S_{hk}|$ and phase φ_{hk} are encoded *via* the circle radius and hue (top) and the centroidal distance and direction (bottom). In the latter case the S_{hk} is directly related to the varying uniformity of distribution, highlighted by the cyclotomic point sets. Note that along the special directions $[h0]$ and $[0k]$ the cyclotomic point sets represent the individual behaviour of the x and y coordinates of the points, which show perfect equidistribution corresponding to their construction from multiples of 1/16.

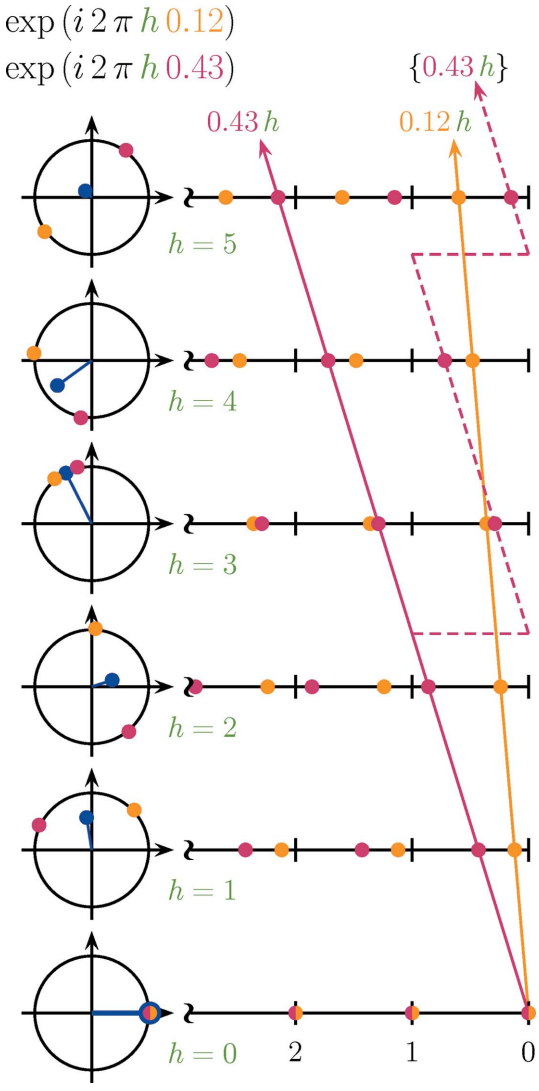

Figure 8
Weyl sum representation of structure factors II: shown are graphical depictions of the Weyl sums for a set of two points and with h ranging from $h = 0$ to $h = 5$ and a corresponding linearization. The determination of the x coordinates of the points (a 'structure solution') is transformed from a uniform distribution problem stated on the complex unit circle and in terms of phase angles into an equivalent one stated on the real number line and in terms of linear slopes. Here, $\{x_j h\}$ denotes the fractional (*i.e.* modulo one) part of $x_j h$, a straight line of slope x_j in the variable h (one such line is highlighted by dashes). Note that the depicted example represents the very simple case of a one-dimensional, equal-atom structure with atomic form factor set to unity and therefore differs from that of an actual crystal structure and its corresponding diffraction pattern.

sponding reflection *hkl* to be strong, *i.e.* having a large structure-factor amplitude $|F_{\mathbf{h}}|$. Moreover, if the collection of atoms (points) exhibits a perfect sublattice structure, only a few net planes will fulfil this condition; hence only a few reflections will collect all the intensity (compare Fig. 5), and the spectral test rather than the diaphony is the appropriate measure of uniform distribution.

The same observation is true, in principle, for a general set of atoms (points), although one has to keep in mind that the diaphony is a global measure of uniform distribution and, by its very definition as an average rather than a worst-case quantity (*i.e.* as an L^2 rather than L^∞ norm), is therefore affected by all kinds of subtle spatial correlations being present in the set of atoms (points) under consideration. Notwithstanding these limitations, a non-trivial conclusion can be drawn from a trivial fact. As every crystallographer knows, the intensity modulation of a diffraction pattern in reciprocal space represents a real-space atomic distribution, yet, and more specifically, it also is a measure of its spatial *uniformity*, eventually yielding the diaphony measure of the mathematician.

In particular, the phasor description of the structure factor is related to the geometric interpretation of the Weyl sums used in the definition of the diaphony (Fig. 7). That is to say, if a given reflection *hkl* is strong, its Weyl sum representation, too, exhibits strong deviations from a uniform distribution.

The plot thereby connects a structure factor's complex amplitude and phase with the equidistribution properties of point sets on the complex unit circle – akin to the cyclotomic points sets discussed by Patterson (1944) – in which the specific locations of the points are ultimately associated, *via* a weighted variant of the Weyl sum, with a crystal structure's atomic coordinates (Fig. 8)![1]

7. Zinterhof's diaphony and the Patterson function

As a matter of fact, a mathematically equivalent definition of the diaphony exists, namely

$$F_N(P) = \left[\frac{1}{N^2}\sum_{\mu=1}^{N}\sum_{\nu=1}^{N} K(\mathbf{x}_\mu - \mathbf{x}_\nu) - 1\right]^{1/2} \qquad (17)$$

in the case of unit weights (Zinterhof, 1976), and

$$F_N(P) = \left[\sum_{\mu=1}^{N}\sum_{\nu=1}^{N} \rho_\mu \rho_\nu \cdot K(\mathbf{x}_\mu - \mathbf{x}_\nu) - \rho^2\right]^{1/2} \qquad (18)$$

in the case of variable weights (Lev, 1995), with $\rho = \sum_{j=1}^{N} \rho_j$ the sum of all weights and

$$K(\mathbf{x}) = \prod_{j=1}^{d}\left[1 + 2\pi^2 B_2(\{x_j\})\right]. \qquad (19)$$

Here, $B_2(x) = x^2 - x + 1/6$ is the second *Bernoulli polynomial*, while $\{x_j\}$ denotes the fractional (modulo one) part of the coordinate x_j.

Skipping the mathematical details for the moment, and focusing on the crystallographic interpretation instead, one has to note that the above definition of the diaphony solely

[1] Note that in an actual diffraction experiment some additional complication arises from the precise distribution of distinct atomic species, differing in their electron count and thus their X-ray scattering cross section, thereby resulting in contorted contributions of subsets of points to the structure-factor amplitudes. In particular, three (interrelated) effects have to be considered: (i) the replacement of unit weights $1/N$ by atomic form factors f_j, (ii) their distinct normalization to unity or some other value, and (iii) their (in)dependence on the scattering vector. These effects alter the geometric interpretation of the Weyl sum and the associated problem of uniform distribution, eventually yielding the structure factor.

depends on real-space difference vectors $\mathbf{x}_\mu - \mathbf{x}_\nu$. Thus, the number-theoretic concept of diaphony is closely related to Patterson's approach of structure solution (Patterson, 1934, 1935; Rossmann & Arnold, 2006) and, in particular, to the Patterson function

$$P(\mathbf{u}) = \frac{1}{V}\sum_{\mathbf{h}\in\Lambda^*} e_{\mathbf{h}}(\mathbf{u})^{-1}\cdot\left|F_{\mathbf{h}}\right|^2, \tag{20}$$

in which $\mathbf{u} = (u, v, w)$ denotes a general real-space vector [compare equation (16)]. Relying solely on intensities, *i.e.* $|F_{\mathbf{h}}|^2$, as experimental observables, it addresses the phase problem of crystallography to the effect of yielding an interatomic distance vector map, in which relative interatomic distances and directions, occurring in a crystal structure, are preserved, while information about the exact position of the atoms and the absolute structure is lost. Since $|F_{\mathbf{h}}|^2 = F_{\mathbf{h}}\cdot F_{-\mathbf{h}}$, where $F_{-\mathbf{h}}$ denotes a complex conjugate, and the Fourier transform of a product is related to a convolution ($*$), the Patterson function can be expressed as the *autocorrelation function* of the electron density: $P(\mathbf{u}) = \varrho(\mathbf{x}) * \varrho(-\mathbf{x})$.

Although equation (20) seems to recover some of the functional relationship of the Weyl sum or Zinterhof's diaphony, it is clear that the term $e_{\mathbf{h}}(\mathbf{u})^{-1}$ does not obey the conditions for proper outer weights as demanded and stated before (compare Appendix *A*).

Yet, a probabilistic interpretation may be given to the Patterson function, namely that of a probability distribution quantifying the frequency of occurrence of a given interatomic distance vector. The diaphony as a scalar quantity is then conceived as a characteristic number obtained by averaging the kernel $K(\mathbf{x})$ with respect to this distribution. In this sense the diaphony represents an *expectation value* of the autocorrelation function and as such resembles similar quantities, such as moments or cumulants, which are commonly used to characterize the shape of a distribution [see Prince (2004), pp. 69–72, for a crystallographic application with respect to the structure-factor equation].

Thus, while the diaphony is not directly related to the Patterson function, it shares some of its essential features, due to its dependence on relative instead of absolute positions, summarizing the (uniform) distribution of interatomic distances within a single quantifier. Furthermore, the mathematical equivalence of Zinterhof's two definitions for the diaphony establishes the exact numerical correspondence, *via* Bernoulli polynomials, between the dual-space intensity distribution and the real-space distance set viewpoints [equations (4) and (17), respectively].

Finally, one should note that the diaphony is an invariant of *homometric* structures (Patterson, 1944), as is the case for the squared structure factors $|F_{\mathbf{h}}|^2$, since homometric structures are characterized by sharing the same interatomic distance vector set (including multiplicities) despite being neither congruent nor enantiomorphic to each other.

8. A crystallographic diaphony

Combining the aforementioned definitions of Lev's diaphony into a single expression and rephrasing it in crystallographic notation yields

$$\frac{\sum_{\mathbf{h}\in\Lambda^*} r(\mathbf{h})^{-2}\cdot\left|F_{\mathbf{h}}\right|^2}{\sum_{\mu=1}^{N}\sum_{\nu=1}^{N} f_\mu f_\nu\cdot K\left(\mathbf{x}_\mu - \mathbf{x}_\nu\right) - f^2} = 1, \tag{21}$$

again introducing atomic form factors as the crystallographically appropriate weights (where $f = \sum_{j=1}^{N} f_j$).

As noted above, this equation is strictly valid only for the ideal case of point scatterers, whereas otherwise the summations in the denominator have to be replaced by integrals in order to account for the dependency of the atomic form factors on $(\sin\theta)/\lambda$. Alternatively, the atomic form factors could be treated as constants, *e.g. via* replacing the f_j by the corresponding atomic numbers, since $f_j = Z_j$ for $(\sin\theta)/\lambda = 0$.

The problem of extended atoms is well known for blurring the structural information contained in a Patterson map, and appears even more pronounced in practice due to additional contributions regarding the thermal motion of atoms around their barycentres. In fact, it was already treated by Patterson (1935), who suggested using a modified set of *sharpened* structure factors $|F_{\mathbf{h},\mathrm{sharp}}|^2 = |F_{\mathbf{h}}|^2/\langle f\rangle^2$, where $\langle f\rangle$ is the average scattering factor per electron, defined as

$$\langle f\rangle = \sum_{j=1}^{N} f_j / \sum_{j=1}^{N} Z_j, \tag{22}$$

with Z_j the atomic numbers of the elements involved.

In a way, Zinterhof's mathematically equivalent definitions of the diaphony reflect the fact that the same concept may be described just as well in dual as in real space, with the enumerator and denominator of equation (21), based on a summation over dual-space intensities and real-space interatomic distances, respectively, being in an exact mathematical correspondence.

Thus, with the enumerator known from a diffraction experiment, and the denominator describing the sought-for crystal structure, equation (21) in principle describes the process of structure solution within a single formula, demanding the quotient to converge to unity once the correct structure is established.

Whether this could lead to a practical improvement of current structure solution algorithms based on the Patterson method, *e.g.* by facilitating a novel strategy for peak sharpening, is not clear. It may, however, be suited for the quantitative evaluation of intermediate structure candidates with already established methods of uniform distribution theory, and may also open up a new perspective regarding the way of thought within the field of structure solution methods.

9. Conclusion

Summarizing, we have shown that well known concepts of uniform distribution theory (various notions of the *diaphony* including the spectral test for lattice point sets) match well known concepts of crystallography (the largest interplanar

spacing of a lattice, the structure-factor equation, the Patterson function) most likely not being noticed (?), at least in their full significance, by practitioners in either field, most probably due to the cumbersome issue of speaking different 'languages'.

Envisaged crystallographic corollaries are: (i) the establishment of a connection of the phasor description of the crystallographic structure factor with the geometric interpretation of the Weyl sum taken from uniform distribution theory (see Fig. 7); (ii) the design of a crystallographic diaphony measuring the uniform distribution of atoms in space based on observed diffraction intensities; and (iii) the combination of Zinterhof's mathematically equivalent definitions for the diaphony within a single formula [equation (21)] augmented by its crystallographic interpretation in the realm of crystal structure solution methodology.

APPENDIX *A*
On norms and weights

In the most general way, the L^p norm ($p \geq 1$) of a p-integrable function f on a measure space S with measure μ is defined as the integral

$$\|f\|_p = \left(\int_S |f|^p \, \mathrm{d}\mu \right)^{1/p}. \tag{23}$$

Since Λ^* is a discrete set the integral of equation (23) is replaced by a sum in equation (4).

For $p \to \infty$ one obtains the special case of the L^∞ norm

$$\lim_{p\to\infty} \|f\|_p = \|f\|_\infty = \sup_{x\in S} |f(x)|, \tag{24}$$

with the supremum denoting the least upper bound. In many practical cases the supremum of a set simply coincides with its maximum, that is to say in those cases where the supremum itself is a part of the set. Moreover, and colloquially speaking, the L^∞ norm describes the worst-case behaviour, whereas the L^2 norm gives an averaged estimate on the uniformity of distribution (Matoušek, 2010).

Natural generalizations of Zinterhof's diaphony concern the choice of the L^p norm and the application of different weighting schemes, aside from applying distinct function systems other than trigonometric, *e.g.* by considering Walsh instead of Fourier basis functions. Note that there are *two* sets of weights involved in the definition of the diaphony, which should not be confused: one set with respect to the Weyl sum, which could be termed *inner* weights, *e.g.* $1/N$ as in equation (2), another one regarding the expression of the L^p norm, which could be termed *outer* weights, *e.g.* $r(\mathbf{h})^{-2}$ as in equation (4), accordingly.

These outer weights may be chosen at will, say according to some specified global properties of the diaphony in mind [Hameren *et al.* (1997) discuss various possibilities], albeit in such a way as to guarantee a sufficiently fast decline regarding the contributions of higher Fourier modes. In particular, one demands the outer weights fulfil the following criteria: (i) $r(\mathbf{h}) > 0$ for all $\mathbf{h}$; (ii) $r(\mathbf{0}) = 1$; and (iii) $\sum_{\mathbf{h}} r(\mathbf{h})^{-2} < \infty$ (see, *e.g.*, Hellekalek & Larcher, 1998, p. 90).

APPENDIX *B*
On the equivalence of the diaphony definitions

The classical diaphony of Zinterhof appears in a twofold form, as stated in the seemingly unrelated equations (4) and (17), or, in the generalization of Lev, equations (14) and (18), respectively. Transcribed into crystallographic terms, combined into the single equation (21), this alleged dichotomy was all the more accentuated by invoking the contrasting perceptions of real and reciprocal space. Naturally, both representations are connected, and their equivalence is demonstrated by the fact that the Bernoulli polynomials can be replaced by their Fourier series expansion:

$$B_2(x) = \frac{1}{2\pi^2} \sum_{h\neq 0} \frac{\exp(i2\pi h x)}{h^2}. \tag{25}$$

Thus, after some algebraic rearrangements, the kernel of equation (21) may be restated as

$$K(\mathbf{x}_\mu - \mathbf{x}_\nu) = 1 + \sum_{\mathbf{h}\in\Lambda^*} r(\mathbf{h})^{-2} \cdot e_{\mathbf{h}}\big(\{\mathbf{x}_\mu - \mathbf{x}_\nu\}\big). \tag{26}$$

Note that one may also introduce a splitting of terms according to

$$e_{\mathbf{h}}\big(\{\mathbf{x}_\mu - \mathbf{x}_\nu\}\big) = e_{\mathbf{h}}\big(\mathbf{x}_\mu\big) e_{\overline{\mathbf{h}}}(\mathbf{x}_\nu), \tag{27}$$

thus performing the summation over independent atomic positions rather than their interatomic distances (where $\overline{\mathbf{h}} = -\mathbf{h}$, hence denoting a complex conjugate in the exponential). Some further calculation and final rearrangement of terms prove the identity of the denominator with the numerator [since the summations over the $e_{\mathbf{h}}(\mathbf{x}_j)$'s always include all atomic positions and the aforementioned splitting emphasizes the squaring of a complex number by multiplication with its complex conjugate].

References

Baake, M. & Grimm, U. (2011). *Z. Kristallogr.* **226**, 711–725.
Baake, M. & Grimm, U. (2012). *Chem. Soc. Rev.* **41**, 6821–6843.
Coveyou, R. R. & MacPherson, R. D. (1967). *J. Assoc. Comput. Machin.* **14**, 100–119.
Dick, J. & Pillichshammer, F. (2005). *Math. Comput. Sim.* **70**, 159–171.
Dick, J. & Pillichshammer, F. (2010). *Digital Nets and Sequences – Discrepancy Theory and Quasi-Monte Carlo Integration.* Cambridge: Cambridge University Press.
Hameren, A., van Kleiss, R. & Hoogland, J. (1997). *Comput. Phys. Commun.* **107**, 1–20.
Hellekalek, P. & Larcher, G. (1998). Editors. *Random and Quasi-Random Point Sets. Lecture Notes in Statistics 138.* New York/Berlin/Heidelberg: Springer.
Hellekalek, P. & Niederreiter, H. (1998). *ACM Trans. Model. Comput. Sim. (TOMACS)*, **8**, 43–60.
Hornfeck, W. (2012). *Acta Cryst.* A**68**, 167–180.
Hornfeck, W. (2013*a*). *Acta Cryst.* A**69**, 355–364.
Hornfeck, W. (2013*b*). *Symmetry: Culture and Science*, **24**, 237–256.
Hornfeck, W. & Harbrecht, B. (2009). *Acta Cryst.* A**65**, 532–542.
Hornfeck, W. & Kuhn, P. (2014). *Acta Cryst.* A**70**, 441–447.

Kritzer, P., Niederreiter, H., Pillichshammer, F. & Winterhof, A. (2014). Editors. *Uniform Distribution and Quasi-Monte Carlo Methods – Discrepancy, Integration and Applications. Radon Series on Computational and Applied Mathematics 15*. Berlin: de Gruyter.
Kuipers, L. & Niederreiter, H. (1974). *Uniform Distribution of Sequences*. New York: John Wiley and Sons.
Lev, V. F. (1995). *Acta Math. Hungar.* **69**, 281–300.
Matoušek, J. (2010). *Geometric Discrepancy – an Illustrated Guide* (*Algorithms and Combinatorics 18*). New York/Berlin/Heidelberg: Springer.
Patterson, A. L. (1934). *Phys. Rev.* **46**, 372–376.
Patterson, A. L. (1935). *Z. Kristallogr.* **90**, 517–542.
Patterson, A. L. (1944). *Phys. Rev.* **65**, 195–201.
Prince, E. (2004). *Mathematical Techniques in Crystallography and Materials Science*, 3rd ed. New York/Berlin/Heidelberg: Springer.
Rossmann, M. G. & Arnold, E. (2006). *International Tables for Crystallography*, Vol. B, ch. 2.3, pp. 235–263. Dordrecht: Springer.
Weyl, H. (1916). *Math. Ann.* **77** 313–352.
Zinterhof, P. (1976). *Sitzungsber. Österr. Akad. Wiss. Math.-Natur. Kl. II*, **185**, 121–132.